Band structure dependence of hot-electron lifetimes in a Pb/Cu(111) quantum-well system

S. Mathias,[1,2,*] A. Ruffing,[1] F. Deicke,[1] M. Wiesenmayer,[3] M. Aeschlimann,[1] and M. Bauer[3]
[1]*Department of Physics and Research Center OPTIMAS, University of Kaiserslautern, 67663 Kaiserslautern, Germany*
[2]*JILA, University of Colorado and National Institute of Standards and Technology, Boulder, Colorado 80309-0440, USA*
[3]*Institut für Experimentelle und Angewandte Physik, Universität Kiel, 24098 Kiel, Germany*
(Received 12 November 2009; revised manuscript received 22 January 2010; published 14 April 2010)

The band structure dependence of the inelastic lifetime of electrons is investigated in a Pb quantum-well system on a Cu(111) substrate with femtosecond time- and angle-resolved two-photon photoemission. For a single monolayer of Pb on Cu(111), we find an unoccupied quantum-well state with a free-electron-like parabolic dispersion around the $\bar{\Gamma}$ point and with negative dispersion for finite momentum. Our investigation of this state is a momentum-dependent study of hot-electron lifetimes in a quantum-well system. We demonstrate the importance of intrasubband-scattering processes for the decay of hot electrons at finite momentum. Furthermore, we find that the competition between intersubband- and intrasubband-scattering processes directly induces a momentum anisotropy in the hot-electron lifetimes. This momentum anisotropy is strongly dependent on the specific electronic band dispersion. We compare our findings with previous investigations of ultrafast electron dynamics in model-like surface-state systems and with ultrafast electron dynamics in Pb full-bulk material. Our findings suggest that the peculiar electronic structure of quantum-well systems can be used to tune ultrafast dynamical properties in metals.

DOI: 10.1103/PhysRevB.81.155429 PACS number(s): 73.21.Fg, 73.20.At, 78.47.J−

I. INTRODUCTION

Quantum-well (QW) states evolve by the confinement of electrons in ultrathin metal films.[1] When the thickness of a film is reduced to values comparable to, or smaller than, the electron coherence length, the electronic bulk-band structure evolves into a quantized electron spectrum in the direction perpendicular to the film. The quantization arises from the standing electron-wave pattern supported by the film and depends critically on film thickness. In many of these ultrathin metal films, various solid-state properties show a clear oscillatory behavior that depends on the film thickness known as quantum oscillations or quantum-size effects. This dependence can be directly related to periodic modulations in the electronic QW state spectrum. Examples of quantum-size effects include the chemical reactivity of the metal film's surface,[2–4] oscillations in the electron-phonon coupling,[5–7] and the film's superconducting transition temperature.[8] An understanding of quantum-size effect could be used to control static physical properties of solid-state systems by means of thin-film engineering.

Only recently, however, has attention been paid to dynamical processes and electronic excitations in QW systems.[9–14] Electronic excitations are important for many chemical and physical phenomena, e.g., surface femtochemistry, ultrafast magnetization processes, and carrier multiplication in solar cells. Of particular interest is the lifetime of an electronic excitation. This information is needed for a basic understanding of all kinds of energy dissipation mechanisms after an optical excitation. In bulk metallic electron systems, for instance, the lifetime of optically excited electrons is in the femtosecond range. Many metals show a Fermi-liquid-like behavior; i.e., their lifetime's energetic dependence in metallic bulk materials yields an inverse proportionality to $\tau \propto (E-E_F)^{-2}$.

The first comparison of ultrafast electronic processes of quantized electron systems with bulk electron systems was carried out by Ogawa *et al.* for thin Ag films on a Fe(100) substrate.[9] They demonstrated that the population decay, i.e., the inelastic lifetime, in Ag QW states is faster than in bulk Ag. The faster relaxation of the excited electrons was accounted for with additional decay channels. The additional decay channels, which comprise elastic scattering of electrons from the film to the substrate, arise because of imperfect confinement of the electrons in the Ag film. The imperfect confinement is caused by the only orientational band gap of the Fe(100) substrate.

Recently, Kirchmann and Bovensiepen investigated ultrathin Pb films grown on a Si(111) substrate.[12] In contrast to the study of Ogawa *et al.*, the total band gap in Si ensures a perfect confinement of the electrons in the Pb QW states. Kirchmann and Bovensiepen demonstrated that the quantization of the electronic structure must be considered explicitly to correctly describe electron lifetimes in ultrathin metal films. Furthermore, the relaxation of hot electrons in Pb/Si(111) is governed by the competition between QW intersubband- and intrasubband-scattering processes.

Our angle-resolved investigation of ultrathin Pb films on Cu(111) confirms this basic difference in ultrafast electron dynamics between quantized and bulk electronic structures. Moreover, because of the competition between intersubband and intrasubband scattering, we demonstrate an explicit dependence of the excited electron lifetimes on the dispersion of the QW subbands in the direction parallel to the film.

Our paper is organized as follows: in Sec. II, we provide the experimental details of the photoelectron analyzer and the preparation of the ultrathin Pb films on the Cu(111) substrate. Next, we describe the photoemission techniques and the laser systems that serve as photoemission light sources. In Sec. III we first characterize the electronic structure for different Pb film thicknesses (Sec. III A). Next, we focus on the description of the single monolayer (ML) Pb on the Cu(111) system, for which we carried out our time-resolved

photoemission studies. The analysis of the electron dynamics is divided into two parts. First, we discuss the excited-electron lifetimes in the paraboidal free-electron-like part and the sidearm of the QW electronic structure (Sec. III B 1). Second, we compare these findings with the electron lifetimes found in Pb bulk material and with recent theoretical findings for Pb/Cu(111) and Pb/Si(111) (Sec. III B 2). This comparison reveals how the quantization and peculiar electronic band structure of a QW system determine the lifetimes of hot electrons. We summarize our findings in Sec. IV.

II. EXPERIMENTAL DETAILS

Angle-resolved–one-photon photoemission (1PPE), two-photon photoemission (2PPE), and time-resolved–two-photon photoemission (tr-2PPE) studies are performed in a magnetically shielded ultrahigh-vacuum chamber (base pressure $<2\times10^{-10}$ mbar) using a hemispherical electron energy analyzer (PHOIBOS 150, SPECS, 150 mm radius). The analyzer is equipped with a two-dimensional detection unit that allows for parallel detection of the photoemitted electrons over a kinetic-energy range of 2 eV and an emission-angle range of up to $\pm13°$. The analyzer is set to an energy resolution of 20 meV and an angular resolution of 0.3°. The system is also equipped with a low-energy electron diffraction system, which is used to check the surface quality and crystalline orientation of the sample prior to the photoemission experiments.

The sample consists of ultrathin Pb films on a Cu(111) substrate. The Cu(111) substrate is cleaned by repetitive sputtering (10 min, 500 eV) and annealing cycles (15 min, 800 K). An effusion cell is used for the evaporation of different thicknesses of Pb, while the substrate is held at 150 K. Only the fabrication of the 1 ML Pb film on Cu(111) is different. In a first step, more than 1 ML of Pb is deposited on the clean Cu(111) crystal at room temperature. The evaporated Pb grows in Stranski-Kastranov mode forming a complete (4×4) surfactant layer with large three-dimensional islands on top.[15–19] This system is then annealed at a temperature of 600 K causing evaporation of all Pb atoms above a thickness of 1 ML. Note that an annealing temperature of 600 K keeps the compressed nonalloyed phase of the 1 ML (4×4) surfactant system.[18,19] During all measurements, the sample is held at a temperature of 150 K.

We use several photoemission techniques for the investigation of ultrathin Pb films on Cu(111). Figure 1 illustrates the excitation schematics of these photoemission techniques including 1PPE, 2PPE, and tr-2PPE. Conventional 1PPE is used to measure the occupied states from below the Fermi energy. 2PPE spectra contain additional information about the excited-state distribution of unoccupied states between the Fermi and vacuum energies. The tr-2PPE technique is used to gain insight into the excited-state electron dynamics in the QW system.

For the different photoemission techniques, we also use two different mode-locked Ti:sapphire laser systems. The static 1PPE and static 2PPE measurements are performed with the second-harmonic ($h\nu=2.95$ eV) and fourth-harmonic ($h\nu=5.9$ eV) of a narrow-bandwidth laser system

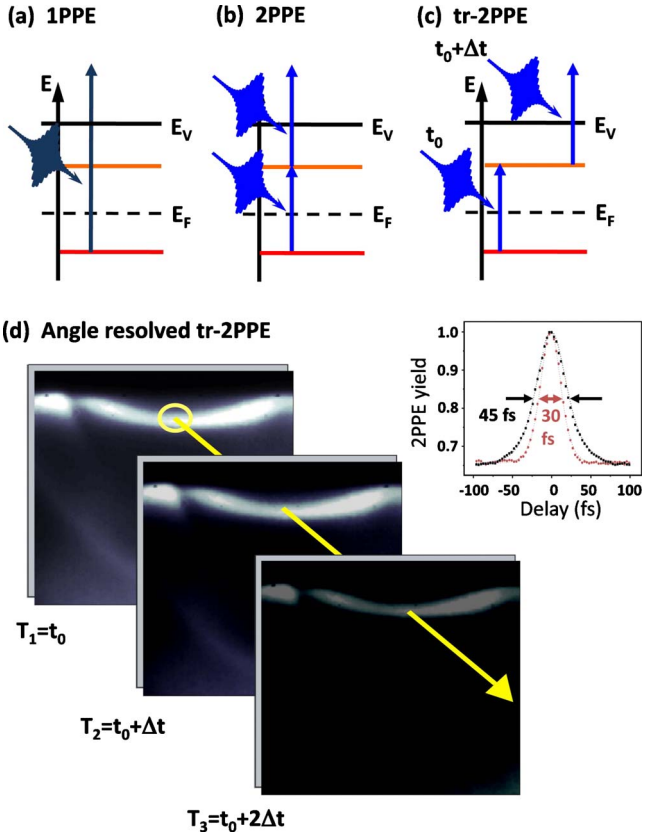

FIG. 1. (Color online) Photoemission methods. (a) Conventional photoemission scheme (1PPE). (b) Two-photon photoemission scheme (2PPE). (c) Time-resolved–two-photon photoemission scheme (tr-2PPE). E_V is the vacuum energy and E_F is the Fermi energy. The red (or dark gray) line depicts an occupied state and the orange (or light gray) line an intermediate unoccupied state. (d) Schematic of the angle-resolved tr-2PPE experiment. $E(k_\parallel)$ photoemission maps are recorded at different temporal delays between the femtosecond pump and probe laser pulse. From this image series, we extract pump-probe autocorrelation traces for each pixel (inset) and finally the lifetime of the hot electron in its $E(k_\parallel)$ state.

(laser 1, bandwidth ≈20 meV, repetition rate: 80 MHz) to ensure high energy resolution.[20] For the time-resolved 2PPE experiments, we use a broad-bandwidth laser system (laser 2, bandwidth ≈100 meV, repetition rate: 76 MHz) that delivers frequency-doubled light pulses of 28 fs temporal width at a photon energy of $h\nu=3.12$ eV.

The tr-2PPE measurements are performed in autocorrelation mode using identical *p*-polarized laser pulses. To eliminate interference contributions to the signal, the data are phase averaged during acquisition using an electric-wobbling motor.

An angle-resolved tr-2PPE scan consists of a series of $E(k_\parallel)$ intensity maps recorded with the two-dimensional energy analyzer at varying temporal delays $(t_0\pm\Delta t)$ between the two laser pulses. Individual 2PPE autocorrelation traces from selected $E(k_\parallel)$ areas are later extracted from these intensity maps [see inset of Fig. 1(d)] and then deconvoluted following an approach described in detail in Ref. 21. This deconvolution procedure finally yields a complete inelastic lifetime value data set, $\tau(E,k_\parallel)$, that covers all of the experi-

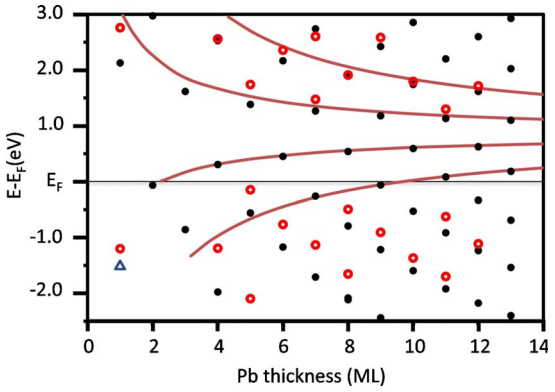

FIG. 2. (Color online) QW subband energies as a function of Pb thickness at normal emission ($\bar{\Gamma}$ point). Lines and black points are theoretical-analytical and density-functional-theory calculations, respectively, as extracted from Ref. 13. The open blue triangle is the energetic position of an occupied QW subband for a free-standing monolayer as extracted from Ref. 25. Open red circles are our experimental data.

mentally accessible energy and momentum range.[22]

The lifetime deconvolution procedure requires an accurate determination of the laser-pulse duration at the sample surface. The laser-pulse duration is extracted by the measurement of the 2PPE autocorrelation trace for excitation from the Cu(111) Shockley surface state.[21,23,24] Finally, the energy and momentum-dependent lifetime variations are color coded and displayed in a two-dimensional $E(k_{\|})$ representation, as discussed below.

III. RESULTS AND DISCUSSION

A. Electronic structure

Using static 1PPE and static 2PPE, respectively, we investigate the occupied and unoccupied electronic structures of ultrathin Pb films on Cu(111) as functions of Pb film thickness. If the Pb film thickness is comparable to or smaller than the electron coherence length, the Pb bulk-band structure quantizes into discrete electronic states. These discrete electronic states are called QW states, or QW subbands, because of their evolution from the original bulk bands. The energetic position and the number of QW subbands in the Pb film strongly depend on the Pb film thickness as shown in Fig. 2 (red or gray circles). We additionally include in Fig. 2 recent analytic (red or gray lines) and density-functional calculations (black dots) of the energetic positions by Zugarramurdi *et al.*[13] For a systematic determination of the energies of the QW subbands in the occupied and unoccupied regime, we evaporated a Pb wedge onto the Cu(111) substrate. The measured energies were then postassigned to Pb-film thicknesses following a best fit to the available theoretical data.[13,25] Because also the energies of the unoccupied QW subbands were taken into account, this procedure results in a +1 ML assignment-shift of our data compared to previous studies where exclusively occupied QW subbands were considered.[12,26–28]

For the 1 ML thick Pb film on Cu(111), we observe an occupied state around $E-E_F=-1.20(1)$ eV and an unoccupied state at about $E-E_F=2.76(1)$ eV. In our angle- and time-resolved 2PPE study, we focus on this 1 ML Pb on Cu(111) film. Here, the quality of the film and, consequently, the quality of the electronic structure are better compared to our thicker films, because the film's fabrication process is different (see Sec. II).

The electronic states at $E-E_F=-1.20(1)$ and $E-E_F=2.76(1)$ eV in the 1 ML Pb film on Cu(111) must be QW electronic subbands of the bulk Pb electronic structure. The two states are energetically located within the Pb bulk parent electronic band. This is in contrast to surface states, which would arise as split-off states of the bulk electronic structure in the oriented band gap. Also, the measured electronic structure for 1 ML is remarkably similar to QW states in quasi-free-standing Pb films[29] and also similar to our recent work on the surfactant layer of Bi/Cu(111).[32] There, we could show that the wave functions of the two states in the 1 ML system are localized inside the overlayer structure, as is expected for QW subbands and in contrast to surface states, which are mainly located outside the crystal in the vacuum side. Of course, the states are not perfectly identical to QW subbands seen in free-standing films or thicker overlayers because of the interaction with the underlying substrate. But, as can be seen by comparison with the work of Dil *et al.* on quasi-free-standing Pb films[29] and by comparison of the energetic positions with the theoretical calculations shown in Fig. 2, the bulk-parent band is already for 1 ML Pb on Cu(111) fairly well reproduced. In thick overlayer quantum wells the reproduction of the bulk-parent band is even more accurate, since boundary effects are less noticeable than in the case of 1 ML coverage. However, our 1 ML Pb film on Cu(111) is the beginning of the QW overlayer sequence and clearly exhibits a QW electronic structure.

The static angle-resolved spectra of the occupied and unoccupied QW subbands in the 1 ML Pb film are displayed in Fig. 3. For generation of the full-angle distribution from −45° to +45°, a tilting of the sample with respect to the analyzer and laser light source is required.[43] Tilting results in a modification of the effective polarization of the laser light impinging on the sample surface and leads to the observed strong asymmetry in the photoemission yield of the spectra.

The 1PPE map is measured with a photon energy of $h\nu=5.9$ eV and shows the $E(k_{\|})$ occupied electronic structure from below the Fermi level. The occupied QW subband exhibits a free-electron-like paraboidal dispersion in the direction parallel to the surface.

The 2PPE map is recorded with $2*h\nu=2.95$ eV, so that we also see the unoccupied electronic structure from above the Fermi level. In comparison to the 1PPE map, the occupied QW subband is still visible but with much lower intensity. All additional electronic structure originates from intermediate states in the unoccupied regime between the Fermi and vacuum level. The unoccupied QW subband also shows a free-electron-like paraboidal dispersion around the $\bar{\Gamma}$ point. However, at higher momenta >0.2 Å^{-1} ($>20°$ emission angle), this QW subband diverges from the simple paraboidal structure into a downward-dispersing sidearm.[30,31] Additionally, the sidearm emerges in a double structure because of quantum-well-induced–Rashba-type–spin-orbit splitting of

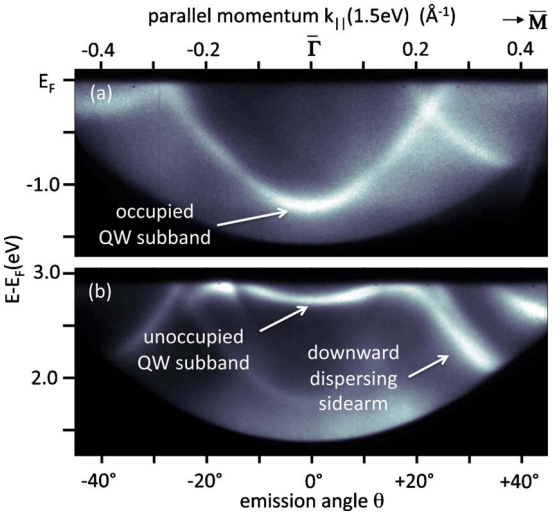

FIG. 3. (Color online) Electronic structure of 1 ML Pb on Cu(111) measured in $\Gamma-M$. (a) 1PPE map recorded with $h\nu=5.9$ eV and (b) 2PPE map recorded with $2*h\nu=2.95$ eV. The energy scale for (b) refers to the unoccupied states only. The band bottoms of the occupied and unoccupied QW states in (a) and (b) are marked with white arrows. Note that for generation of the full-angle distribution a tilting of the sample with respect to the analyzer and laser light source is required. Tilting results in a modification of the effective polarization of the laser light impinging on the sample surface and leads to the observed strong asymmetry in the photoemission yield of the spectra.

this QW subband (i.e., there are two downward-dispersing bands parallel to each other).[32]

Note that the electronic structure of the surfactant layer Pb on Cu(111) has previously been investigated with photoemission by Baumberger *et al.* and no QW subbands could be observed in the 1 ML regime.[33] In this work, however, He Iα radiation with an energy of $h\nu=21$ eV was used. For verification, we also measured the 1 ML Pb/Cu(111) system using He Iα radiation (not shown) and we did not observe any QW subband in consistence with the results by Baumberger *et al.* We conclude that the photon energy of He Iα radiation, $h\nu=21$ eV, exhibits a vanishing photoemission cross section for the QW subbands in contrast to photoemission using $h\nu=6$ eV.

B. Electron dynamics

Using angle-resolved tr-2PPE allows for a parallel imaging of the energy and momentum dependence of hot-electron lifetimes on a specific electronic band structure by means of two-dimensional lifetime maps. To do this, we first create autocorrelation maps that consist of the full width at half maximum (FWHM) of the measured autocorrelation for rectangular areas $\Delta E*\Delta\theta$ in a defined kinetic-energy and momentum range. A reasonable choice of ΔE and $\Delta\theta$ must be determined by comparing the experimental energy and angle resolution with the achievable time resolution. Here we choose $\Delta E=40$ meV and $\Delta\theta=1°$ to compare with the ≈ 100 meV and 0.3° experimental resolutions. An improvement of our time resolution and a smoothing of the extracted

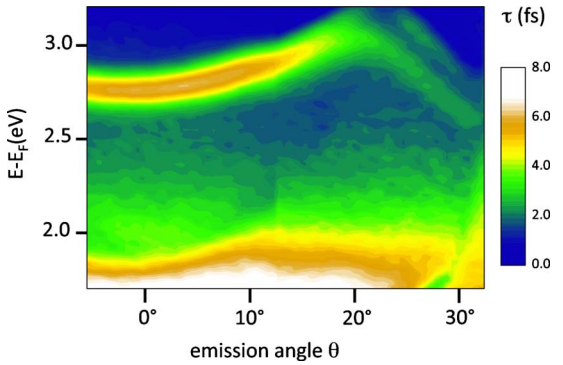

FIG. 4. (Color online) Inelastic lifetime map $\tau(E,k_{\|})$ in the QW subband derived from an angle-resolved tr-2PPE measurement. The lifetime τ is color coded as a function of energy E and parallel momentum $k_{\|}$. A color tone corresponds to 100 as. Note that the extracted inelastic lifetime values in Figs. 5 and 6 are averaged over six of these angle-resolved tr-2PPE measurements.

autocorrelation FWHM values are achieved by semioverlapping the rectangular areas $\Delta E*\Delta\theta$ with their nearest neighbors; i.e., we evaluate $\Delta E*\Delta\theta=(40\ \text{meV})*(1°)$ squares on a grid of $\Delta E'=20$ meV and $\Delta\theta'=0.5°$. Finally, the inelastic lifetime of the electrons is deduced from this autocorrelation map as described in Sec. II.

Figure 4 shows the lifetime map $\tau(E,k_{\|})$ of the unoccupied QW subband as a function of energy E and parallel momentum $k_{\|}$. We can identify the full QW subband, the paraboidal structure, and the downward-dispersing sidearms. The intensities in the color code depict the lifetime of the electrons and our measurement clearly demonstrates a strong dependence of electron lifetimes on the dispersion of the QW subband.

In the following, we first concentrate on the electron dynamics in the unoccupied QW subband (Sec. III B 1). Second, we compare our findings to recently available calculations[13] and to electron dynamics in Pb bulk material (Sec. III B 2).

1. Dynamics in the 1 ML Pb/Cu(111) QW subband

The paraboidal structure $E\propto k_{\|}^2$ found around the $\bar{\Gamma}$ point for the unoccupied QW subband in the 1 ML Pb on Cu(111) system is similar to the intensively studied Shockley and image-potential surface states.[34–38] Therefore, we can compare our findings with known band structure dependencies of hot-electron lifetimes in surface-state systems. However, neither a theoretical momentum-dependent study nor an experimental momentum-dependent study of electron lifetimes in a QW system has been carried out so far.

In all previously investigated surface-state systems, the competition between interband- and intraband-scattering processes determines the band structure dependence of hot-electron lifetimes. In the case of QW systems, the analogous processes are called intrasubband and intersubband scatterings.

In both intrasubband and intersubband scatterings, a hot electron relaxes its energy via Coulomb scattering with a second electron in a different band that is below the Fermi

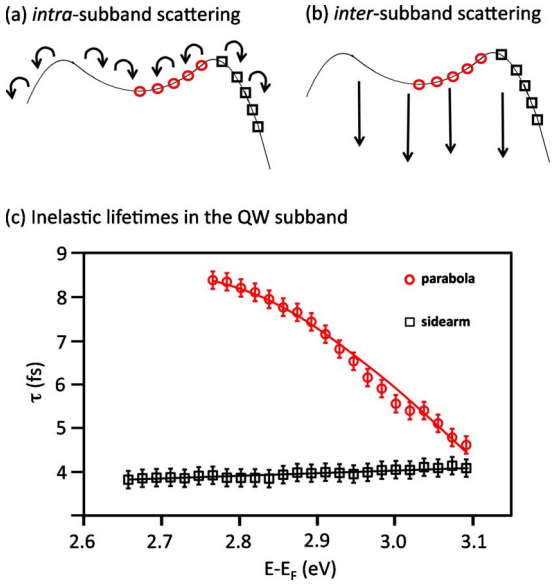

FIG. 5. (Color online) Electron dynamics in the QW subband. [(a) and (b)] Schemes of intrasubband- and intersubband-scattering processes, respectively. (c) Extracted inelastic lifetimes of the paraboidal QW structure (red circles) and the downward-dispersing sidearm (black data) as a function of energy $E-E_F$. Lines serve as a guide for the eyes. The data are averaged from six separate tr-2PPE measurements. The total error between the six different sets is ± 1.5 fs. The (relative) errors bars within one lifetime map are shown in the graph; they are below ± 200 as.

level. The second electron gains the energy and momentum of the hot electron and is excited into an unoccupied state (Auger-like process). For intraband-scattering processes, initially excited electrons remain inside the QW subband but change their momentum and cascade energetically down toward the specific band minimum [Fig. 5(a)]. In interband-scattering processes, the initially excited electrons scatter into different QW subbands [Fig. 5(b)].

Our momentum-dependent observations of hot-electron lifetimes in the paraboidal part of the QW subband are very similar to the case of hot-electron lifetimes in image-potential states of Cu(100).[38] In the case of image-potential states, intraband- and interband-scattering processes are equally important for the relaxation of the excited electrons. As with our observations for the QW subband, the lifetimes in the parabolic image-potential states are strongly momentum dependent and the longest lifetime is found at the band bottom (see lifetime map, Fig. 4).

For a detailed analysis, we extract and display the lifetime values in the QW band as a function of energy $E-E_F$ [Fig. 5(c)]. The extracted lifetime values are averaged over six separate angle-resolved tr-2PPE measurements. The total error after averaging these six separate sets is ± 1.5 fs. The error results predominantly from the accuracy of the measured laser-pulse duration at the sample surface that is required for the deconvolution procedure of the inelastic lifetimes.[23,24] Within one lifetime map (one measurement), the laser-pulse duration is equal for all extracted $\tau(E,k_{\|})$ inelastic lifetime values. Therefore, we are able to determine the lifetimes within one lifetime map with an exceptional low relative error. The relative error is found to be ± 200 as.

Coming back to the discussion of intrasubband- and intersubband-scattering processes in the 1 ML Pb/Cu(111) system, we find it interesting to compare the hot-electron lifetime at the band bottom of the parabolic part ($\bar{\Gamma}$ point) with the lifetime at finite momentum in the downward-dispersing sidearm of the QW subband at the same excitation energy $E-E_F$. Electrons located in the subband bottom can relax their energy only by intersubband-scattering processes, in contrast to electrons in the sidearm, for which both intrasubband- and intersubband-scattering channels are available.

At the $\bar{\Gamma}$ point, we find an increased lifetime value of 8.4 fs because of the complete suppression of intraband-scattering processes. The corresponding lifetime at the same energy in the sidearm is only 3.9 fs. By neglecting an additional momentum dependence, we can roughly estimate the ratio of intersubband-to-intrasubband decay rates Γ (inverse lifetimes) in the sidearm to be

$$\frac{\Gamma_{\text{interband}}}{\Gamma_{\text{intraband}}} = \frac{\tau_{\text{intraband}}}{\tau_{\text{interband}}} \approx 1. \quad (1)$$

Intrasubband and intersubband scatterings are apparently competitive and equally important processes for the relaxation of excited electrons in the sidearm. They also determine the dependence of hot-electron lifetimes $\tau(E,k_{\|})$ on the dispersion of the QW subband. Beginning in the subband bottom at the $\bar{\Gamma}$ point, we see that for energies and momenta in excess of the energy in the QW band bottom, the probability of electrons relaxing their energy by intraband scattering toward the QW-state-band minimum increases because of the increased number of final states. The lifetime consequently decreases to a value of ≈ 4.5 fs at the highest intermediate-state energy. At even higher momenta, however, the QW subband diverges from its paraboidal free-electron-like structure into the sidearm structure and the dynamical properties of the excited electrons alter as well. Note that the downward-dispersing sidearm clearly extends toward lower energies and higher momenta even beyond the cutoff of our 2PPE measurement (Fig. 3). In agreement with our argumentation of competitive intrasubband and intersubband scatterings, we do not observe an increase in lifetime toward lower energies as seen for the paraboidal part of the subband and expected for Fermi-liquid-like behavior.

2. Comparison of electron dynamics between Pb QW and Pb bulk material

Since the quantization of the electronic structure in the ultrathin Pb film induces a strong momentum dependence, we want to compare this finding with the situation in full Pb material, where the bands are completely formed. To do this comparison, we evaporate Pb with a thickness of about 100 nm onto the Cu(111) substrate. The Pb film thickness is much larger than the electron coherence length and the bulk bands are therefore completely formed in all **k** directions.

Figure 6(a) shows a 2PPE photoemission spectrum of bulk Pb recorded with laser 2 ($h\nu=3.12$ eV). No electronic features can be observed in the relevant energy range. Con-

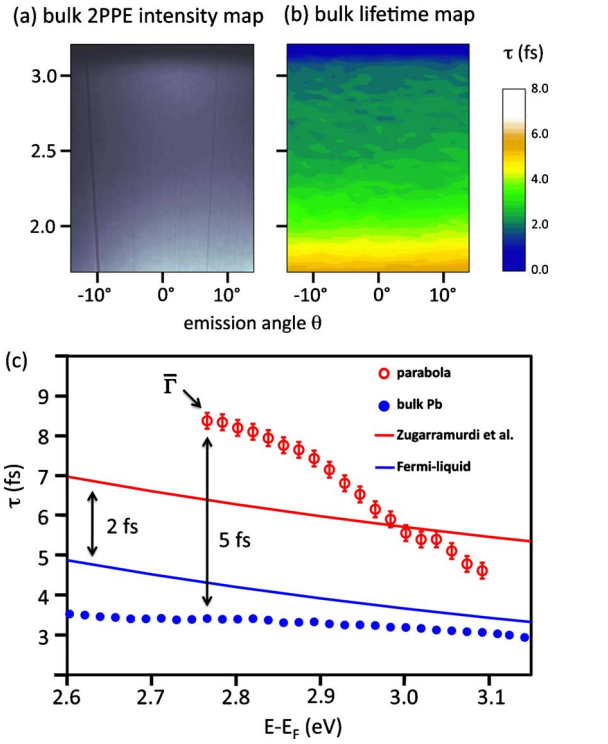

FIG. 6. (Color online) Electron dynamics in Pb bulk material. (a) 2PPE intensity map of 1 ML Pb/Cu(111) in comparison to (b) lifetime map of Pb bulk material. (c) Experimental inelastic-lifetime values of the QW parabola (red circles) and Pb bulk material (blue dots). Lines: theoretical data derived by Zugarramurdi *et al.* (Ref. 13) for quantized-Pb systems (red line) and theoretical data describing Pb bulk material, as derived by Fermi-liquid theory (blue line) (Ref. 39). Note that theoretical data are calculated only for the $\bar{\Gamma}$ point.

sequently, a momentum-dependent anisotropy in the derived lifetime map [Fig. 6(b)] of the Pb bulk system is completely absent. We observe only a weak energetic dependence of the lifetimes toward lower energies.

Both observations are expected. The momentum anisotropy is caused by the quantization of the bands that leads to a suppression of intrasubband-scattering processes. In the full-bulk structure, however, there are no QW-subband bottoms present. Thus, the bulk band disperses continually in the direction perpendicular to the film. Electrons in the bulk structure can relax their energy by both intraband- and interband-scattering processes in all possible **k** directions.

Theoretically, electron lifetimes in many metallic bulk systems can approximately be described with a Fermi-liquid-like behavior that yields an inversely proportional quadratic dependence of the electron lifetime τ on the electron energy $\tau \propto (E-E_F)^{-2}$. The inelastic lifetime of excited electrons and holes in a homogeneous free-electron gas as derived with Fermi-liquid theory by Quinn and Ferell[39] is

$$\tau \approx \hbar/(2.5019 r_s^{5/2}[(E-E_F)^2]). \quad (2)$$

Here, we use the density parameter $r_s=2.3$ a.u., which corresponds to bulk Pb.

The Fermi-liquid theory [blue line, Fig. 6(c)] fits reasonably to our experimental data for bulk Pb [blue dots, Fig. 6(c)]. The lifetime τ smoothly increases toward lower energies and the absolute values fit within the error (± 1.5 fs). Our measurement of bulk Pb is also consistent with recent combined-experimental and *ab initio*-theoretical work by Hong *et al.*[14] at the $\bar{\Gamma}$ point. They found the same Fermi-liquid-like behavior for Pb on Si(111). Interestingly, both their measurements and their calculations are carried out for ultrathin Pb QW films and not for Pb bulk material. They found that the inelastic electron lifetimes in QW films at the $\bar{\Gamma}$ point matched the inelastic electron lifetimes in full-bulk Pb material.

Comparing this result with the very strong momentum dependence observed in our QW system, we find that it must be coincidence, or, this finding can only be true at the $\bar{\Gamma}$ point. A Fermi liquid does not show momentum-dependent electron lifetimes because of the isotropy of the system in all **k** directions. Additionally, for other materials, for instance, Yb, a non-Fermi-liquid behavior of hot-electron lifetimes has been found.[40]

Indeed, a deviation from Fermi liquid has also been found theoretically for ultrathin Pb films on a Cu(111) substrate at the $\bar{\Gamma}$ point. Zugarramurdi *et al.*[13] recently calculated (within the GW approximation)[41] hot-electron lifetimes of Pb/Cu(111) as functions of film thickness. In their work, they took explicitly into account the Cu(111) substrate and all band structure effects in the direction perpendicular to the surface, i.e., the quantization of the bulk band structure for ultrathin Pb films. They found Fermi-liquid-like behavior for low excitation energies (<0.5 eV), but considerable deviations at energies above $E-E_F=1$ eV [see Fig. 6(c)]. The deviation was attributed to their more sophisticated theory compared to Fermi-liquid theory. For instance, Zugarramurdi *et al.* used the random-phase approximation in the description of the screening.[41] This approximation does not give a quadratic dependence of the lifetimes for higher energies.

We include the theoretical data of Zugarramurdi *et al.* in Fig. 6(c) (red line). In comparison to our bulk measurement and the Fermi-liquid description, the lifetimes in this energy range are found to be about 2 fs longer. In our experimental data, the increase compared to the lifetimes in bulk Pb is ≈ 5 fs. Furthermore, the difference clearly depends on the electron momentum. We therefore conclude that the lifetime values may incidentally match at the $\bar{\Gamma}$ point or at any other finite momentum, but they cannot be the same for the complete momentum range.

Finally, we address the discrepancy between the longer lifetime value of the 1 ML Pb system in the paraboidal subband bottom of 8.4 fs in comparison to the theoretical data yielding 6.4 fs for the quantized system. For thinner films, Zugarramurdi *et al.* found that an additional spread of the electron-wave function reduces the probability for electron–electron-scattering processes and increases the lifetime.[13] Furthermore, effects such as band folding caused by the lattice mismatch between the Cu surface and the Pb overlayer have not been considered in Ref. 13 and may also affect inelastic electron lifetimes.

Summing up, both experimental and theoretical data sets (Zugarramurdi *et al.*, Ref. 13) show an increase in electron

lifetimes for ultrathin Pb films on Cu(111) at the QW-subband bottoms as compared to our measurement of full Pb bulk material or ultrathin Pb films on Si(111) (Hong *et al.*, Ref. 14). Because of the strong momentum dependence that we observe in the Pb/Cu(111) QW system, we conclude that, in general, electron dynamics in quantized electron systems are different from electron dynamics in the corresponding bulk materials.

IV. SUMMARY AND OUTLOOK

We have investigated the electronic band structure and hot-electron lifetimes in a Pb/Cu(111) QW system. We find that competition of intrasubband- and intersubband-scattering processes is crucial for an accurate description of hot-electron lifetimes in quantized electronic systems. Furthermore, we find that electron lifetimes are not only modified because of the quantization of the electronic bands,[12,13] but also strongly depend on the specific electronic subband structure in the direction parallel to the surface. The peculiar electronic structure of QW systems can therefore be used to tune ultrafast dynamical properties in electronic systems with reduced dimensions. This tuning ability has direct consequences for possible applications, e.g., in the areas of photo-induced chemical processes on a surface, carrier multiplication in solar cells, and multiple exciton generation in semiconductor quantum dots.[42]

Future studies of this QW system will include an investigation of the observed significantly lower electron lifetimes in the spin-orbit-split second sidearm. In particular, we will consider the effect of the spin-orbit splitting identified for high momentum values [cf. electronic spectrum (Fig. 3) and lifetime map (Fig. 4)]. Here, spin-, angle-, and time-resolved two-photon photoemission studies in combination with theoretical support may provide deeper insight into the Pb/Cu(111) system and spin-dependent electron dynamics in general.

In terms of technique, we have shown that the use of angle-resolved tr-2PPE allows us to create hot-electron lifetime maps with extremely high relative time resolution into the attosecond regime. The combination of angle-resolved photoemission with tr-2PPE opens up future investigations of ultrafast dynamics in considerably more complex electronic systems.

ACKNOWLEDGMENTS

S.M. thanks Luis Miaja-Avila for his support during the initial data-taking process. This work was supported by the Deutsche Forschungsgemeinschaft through Grant No. DFG GRK 792 "Nichtlineare Optik und Ultrakurzzeitphysik" and Grant No. DFG SFB/TRR49 "Condensed Matter Systems with Variable Many-Body Interactions."

*smathias@physik.uni-kl.de

[1] T. Chiang, Surf. Sci. Rep. **39**, 181 (2000).
[2] L. Aballe, A. Barinov, A. Locatelli, S. Heun, and M. Kiskinova, Phys. Rev. Lett. **93**, 196103 (2004).
[3] N. Binggeli and M. Altarelli, Phys. Rev. Lett. **96**, 036805 (2006).
[4] B. Sun, P. Zhang, S. Duan, X.-G. Zhao, and Q.-K. Xue, Phys. Rev. B **75**, 245422 (2007).
[5] D. A. Luh, T. Miller, J. J. Paggel, and T. C. Chiang, Phys. Rev. Lett. **88**, 256802 (2002).
[6] S. Mathias, M. Wiesenmayer, M. Aeschlimann, and M. Bauer, Phys. Rev. Lett. **97**, 236809 (2006).
[7] S. Mathias, S. V. Eremeev, E. V. Chulkov, M. Aeschlimann, and M. Bauer, Phys. Rev. Lett. **103**, 026802 (2009).
[8] M. M. Özer, Y. Jia, Z. Zhang, J. R. Thompson, and H. H. Weitering, Science **316**, 1594 (2007).
[9] S. Ogawa, H. Nagano, and H. Petek, Phys. Rev. Lett. **88**, 116801 (2002).
[10] E. V. Chulkov, J. Kliewer, R. Berndt, V. M. Silkin, B. Hellsing, S. Crampin, and P. M. Echenique, Phys. Rev. B **68**, 195422 (2003).
[11] D. Wegner, A. Bauer, and G. Kaindl, Phys. Rev. Lett. **94**, 126804 (2005).
[12] P. S. Kirchmann and U. Bovensiepen, Phys. Rev. B **78**, 035437 (2008).
[13] A. Zugarramurdi, N. Zabala, V. M. Silkin, A. G. Borisov, and E. V. Chulkov, Phys. Rev. B **80**, 115425 (2009).
[14] I.-Po Hong, C. Brun, F. Patthey, I. Y. Sklyadneva, X. Zubizarreta, R. Heid, V. M. Silkin, P. M. Echenique, K. P. Bohnen, E. V. Chulkov, and W. D. Schneider, Phys. Rev. B **80**, 081409(R) (2009).
[15] J. Henrion and G. Rhead, Surf. Sci. **29**, 20 (1972).
[16] S. Muller, J. Prieto, C. Rath, L. Hammer, R. Miranda, and K. Heinz, J. Phys.: Condens. Matter **13**, 1793 (2001).
[17] C. de Beauvais, Y. Girard, C. Perard, B. Croset, and B. Mutaftschiev, Surf. Sci. **367**, 129 (1996).
[18] G. Meyer, M. Michailov, and M. Henzler, Surf. Sci. **202**, 125 (1988).
[19] B. Muller, T. Schmidt, and M. Henzler, Surf. Sci. **376**, 123 (1997).
[20] J. Koralek *et al.*, Phys. Rev. Lett. **96**, 017005 (2006).
[21] J. P. Gauyacq and A. K. Kazansky, Phys. Rev. B **72**, 045418 (2005).
[22] S. Mathias, M. Wiesenmayer, F. Deicke, A. Ruffing, L. Miaja-Avila, M. M. Murnane, H. C. Kapteyn, M. Bauer, and M. Aeschlimann, J. Phys.: Conf. Ser. **148**, 012042 (2009).
[23] T. Hertel, E. Knoesel, M. Wolf, and G. Ertl, Phys. Rev. Lett. **76**, 535 (1996).
[24] F. Steeb, S. Mathias, A. Fischer, M. Wiesenmayer, M. Aeschlimann, and M. Bauer, New J. Phys. **11**, 013016 (2009).
[25] C. M. Wei and M. Y. Chou, Phys. Rev. B **66**, 233408 (2002).
[26] R. Otero, A. L. Vazquez de Parga, and R. Miranda, Phys. Rev. B **66**, 115401 (2002).
[27] J. H. Dil, J. W. Kim, S. Gokhale, M. Tallarida, and K. Horn, Phys. Rev. B **70**, 045405 (2004).
[28] P. S. Kirchmann, M. Wolf, J. H. Dil, K. Horn, and U. Boven-

siepen, Phys. Rev. B **76**, 075406 (2007).
[29] J. H. Dil, T. U. Kampen, B. Hülsen, T. Seyller, and K. Horn, Phys. Rev. B **75**, 161401(R) (2007).
[30] M. H. Upton, T. Miller, and T. C. Chiang, Phys. Rev. B **71**, 033403 (2005).
[31] J. H. Dil, J. W. Kim, T. Kampen, K. Horn, and A. R. H. F. Ettema, Phys. Rev. B **73**, 161308(R) (2006).
[32] S. Mathias, A. Ruffing, F. Deicke, M. Wiesenmayer, I. Sakar, G. Bihlmayer, E. V. Chulkov, Y. M. Koroteev, P. M. Echenique, M. Bauer, and M. Aeschlimann, Phys. Rev. Lett. **104**, 066802 (2010).
[33] F. Baumberger, A. Tamai, M. Muntwiler, T. Greber, and J. Osterwalder, Surf. Sci. **532-535**, 82 (2003).
[34] T. Fauster, M. Weinelt, and U. Hoefer, Prog. Surf. Sci. **82**, 224 (2007).
[35] J. Kliewer, R. Berndt, E. Chulkov, V. Silkin, P. Echenique, and S. Crampin, Science **288**, 1399 (2000).
[36] P. Echenique, R. Berndt, E. Chulkov, T. Fausterd, A. Goldmann, and U. Höfer, Surf. Sci. Rep. **52**, 219 (2004).
[37] L. Vitali, P. Wahl, M. Schneider, K. Kern, V. Silkin, E. Chulkov, and P. Echenique, Surf. Sci. **523**, L47 (2003).
[38] W. Berthold, U. Höfer, P. Feulner, E. V. Chulkov, V. M. Silkin, and P. M. Echenique, Phys. Rev. Lett. **88**, 056805 (2002).
[39] J. Quinn and R. Ferell, Phys. Rev. **112**, 812 (1958).
[40] V. P. Zhukov, E. V. Chulkov, P. M. Echenique, A. Marienfeld, M. Bauer, and M. Aeschlimann, Phys. Rev. B **76**, 193107 (2007).
[41] P. Echenique, J. Pitarke, E. Chulkov, and A. Rubio, Chem. Phys. **251**, 1 (2000).
[42] A. J. Nozik, Chem. Phys. Lett. **457**, 3 (2008).
[43] We use standard picture panorama software to merge the full-angle distribution photoemission maps from several individual measurements (Figs. 3, 4, and 6). In the process of merging, the data are slightly corrected for lens distortions and intensity deviations. Therefore, all physical quantities shown in our paper are extracted from the original data sets.